

QUANTUM SIMULATIONS WITH  
PHOTONS IN ONE-DIMENSIONAL  
NONLINEAR WAVEGUIDES

MING-XIA HUO

A THESIS SUBMITTED FOR THE  
DEGREE OF DOCTOR OF PHILOSOPHY

CENTRE FOR QUANTUM TECHNOLOGIES  
NATIONAL UNIVERSITY OF SINGAPORE

2013



## DECLARATION

I hereby declare that the thesis is my original work and it has been written by me in its entirety. I have duly acknowledged all the sources of information which have been used in the thesis.

This thesis has also not been submitted for any degree in any university previously.



---

MING-XIA HUO

24 July 2013



---

## Acknowledgments

First and foremost, I am deeply grateful to Kwek Leong Chuan. To work with him has been a real pleasure to me. He has been oriented and supported me with promptness and care. He has always been patient and encouraging in times of new ideas and difficulties. He has also provided insightful discussions and suggestions. I appreciate all his contributions of time, ideas, and funding to make my PhD experience excellent. Above all, he made me feel a friend, which I appreciate from my heart.

Furthermore, I am immensely grateful to Dimitris Angelakis. His high level of comprehension and sharpness on physical subjects have taught me to be rigorous and to tackle aspects of physics with a level of confidence that I never had before. I am also very grateful for his scientific advice and knowledge and many insightful discussions and suggestions.

In addition, I have been very privileged to get to know and to collaborate with David Hutchinson. I learned a lot from him about research, language, how to tackle new problems and how to develop techniques to solve them. He has been a pleasure to work with. Thanks for helping me a lot.

I would also like to give thanks to Wenhui Li for her unwavering support professionally and personally at every important moment of my PhD experience. I will truly miss those discussions and conversations. Thanks for all the good times.

I also had the great pleasure of meeting Christian Miniatura. From the very beginning of my PhD career, he supported me. Thanks for the fun and encouraging discussions over the last several years.

I would like to thank my collaborator Darrick Chang, whose physical understanding in the research area is tremendous and whose scientific work inspired me a lot. Our collaborated work has also benefited from sugges-

---

tions and kind encouragement from Vladimir Korepin. His technical depth and attention to details are amazing. I also want to thank David Wilkowski for providing me the opportunity to have fruitful collaborations with his experimental group in a near future.

I would like to thank the collaborators I had the pleasure to work with. Special thanks to the postdocs Changsuk Noh, Blas M. Rodriguez-Lara, Elica Kyoseva, and the student Nie Wei. They have helped me a lot.

I am grateful to my committee members: Berge Englert, Wenhui Li, and Chorng Haur Sow. I have also immeasurably benefited from the course "Quantum Information and Computation", for which I thank the instructor Dagomir Kaszlikowski.

I wish to thank Rosario Fazio and Davide Rossini for making DMRG available to me. I have been interested in DMRG for a long time, and they provided me with a big help. I also want to thank Kerson Huang for interesting and illuminating discussions when I first started my PhD career.

I am grateful to our physics group members for providing me with the best working environment. In particular, I like to thank Dai Li, Setiawan, Thi Ha Kyaw for their willingness to share their research experience and many helpful information. I also want to thank Chunfeng Wu for her advice, support, and encouragement. A special acknowledgement goes to Hui Min Evon Tan and Ethan Lim, who were very nice and always ready to help.

I will forever be thankful to my former Bachelor and Master Degree advisor Zhi Song. He has been helpful in providing advice many times during my stay there. He remains my best role model for a scientist and teacher. I am also very grateful to Changpu Sun, for his tremendous and

---

invaluable suggestions, advices, inspiration, and guidance. Thanks for all these helps.

This dissertation is dedicated to my father Jujiang Hu, my mother Shulan Chen, my husband Ying Li, and my daughter Daiyao Li, for their infinite support throughout everything. Words cannot express my gratitude of love. A final thanks goes to my friends, not previously mentioned, who supported me and influenced me a lot.





# Contents

<b>Acknowledgments</b>	<b>i</b>
<b>Table of Contents</b>	<b>v</b>
<b>Summary</b>	<b>ix</b>
<b>List of Publications</b>	<b>xi</b>
<b>List of Figures</b>	<b>xiii</b>
<b>List of Symbols</b>	<b>xv</b>
<b>1 Introduction</b>	<b>1</b>
<b>2 Background</b>	<b>9</b>
2.1 Electromagnetic Induced Transparency and Dark-State Polaritons . . . . .	9
2.2 Lieb-Liniger Model and Luttinger Liquid Theory . . . . .	12
2.3 Correlation Functions . . . . .	16
<b>3 Pinning Quantum Phase Transition of Photons</b>	<b>21</b>
3.1 Bose-Hubbard and Sine-Gordon Models . . . . .	21
3.2 Quantum Optical Simulator with One-Species Four-Level Atoms . . . . .	22
3.3 Polaritons Trapped in an Effective Periodic Lattice . . . . .	27
3.4 Reaching Correlated Bose-Hubbard and Sine-Gordon Regimes	30
3.5 Polaritonic/Photonic Pinning Transitions . . . . .	31
3.6 Characteristic First- and Second-Order Correlations of Transitions . . . . .	35

<b>4</b>	<b>Simulating Cooper Pairs with Photons</b>	<b>39</b>
4.1	BCS-BEC-BB Crossover . . . . .	39
4.2	Quantum Optical Simulator with Two-Species Four-Level Atoms . . . . .	42
4.3	Decoherence Analysis . . . . .	48
4.4	Two-Component Bose-Hubbard and Effective Fermi- Hubbard Models of Polaritons . . . . .	50
4.5	Witnesses of BCS-BEC-BB Crossover . . . . .	53
<b>5</b>	<b>Spin-Charge Separation in a Photonic Luttinger Liquid</b>	<b>57</b>
5.1	Spin-Charge Separation . . . . .	57
5.2	From Luttinger Liquid to Spin-Charge Separation . . . . .	59
5.2.1	Bosonization Approach and Single-Component Lieb- Liniger Model . . . . .	59
5.2.2	Two-Component Lieb-Liniger Model and Spin- Charge Separation . . . . .	60
5.3	Spin-Charge Separation with Differently Colored Photons . .	62
5.3.1	Polaritonic Spin-Charge Separation with Two- Species Four-Level Atoms . . . . .	62
5.3.2	Spinon and Holon Velocities . . . . .	71
5.4	Spin-Charge Separation with Differently Polarized Lights . .	76
5.4.1	Polaritonic Spin-Charge Separation with Single- Species Multi-Level Atoms . . . . .	78
5.4.2	Spinon and Holon Velocities . . . . .	82
<b>6</b>	<b>Simulating Interacting Relativistic Quantum Field Theo- ries with Photons</b>	<b>85</b>
6.1	Thirring Model . . . . .	85

## Contents

---

6.2	Photons for Interacting Fermions . . . . .	87
6.3	Nonlinear Dynamics of Relativistic Stationary Polaritons . . . . .	88
6.4	Thirring Model with Stationary Pulses of Light . . . . .	91
6.5	Correlation Scaling . . . . .	96
<b>7</b>	<b>Conclusions and Outlook</b>	<b>99</b>
	<b>Bibliography</b>	<b>105</b>
<b>A</b>	<b>Derivation of Nonlinear Evolution Equation for Single-Species Photons</b>	<b>115</b>
A.1	Atomic Operators . . . . .	115
A.2	Quantum Light Evolution . . . . .	120
<b>B</b>	<b>Derivation of Nonlinear Evolution Equation for Two-Species Photons with Different Frequencies</b>	<b>123</b>
B.1	Atomic Operators . . . . .	123
B.2	Quantum Light Evolution . . . . .	131
<b>C</b>	<b>Derivation of Nonlinear Evolution Equation for Two-species Photons with Different Polarizations</b>	<b>133</b>
C.1	Atomic operators . . . . .	133
C.2	Quantum Light Evolution . . . . .	138



# Summary

The study of one-dimensional (1D) strongly correlated quantum liquids is a fascinating area and has attracted a lot of attention recently. In spite of their apparent conceptual simplicity, both their ground states and excited states exhibit a large number of exotic strong-correlated effects. On the other hand, the achievement of strongly correlated quantum optical systems which accurately describe condensed matter physics and quantum field theory models has opened many new perspectives for research on strongly correlated systems. These quantum optical systems with the most famous examples being optical lattices and ion traps share many features with conventional systems, while several of their properties distinguish them from the traditional setups like, their long coherence times and the ability to control Hamiltonian parameters over a wide range. Recently, the 1D optical nonlinear waveguide as a promising optical system with a tight field confinement and coherent photon trapping techniques has been proposed, where the dark-state polaritons are formed as a combination of light and matter excitations. Their highly nonlinear behavior has provided a platform to enable amazing experiments in the field on quantum nonlinear optics and slow-light applications. It is the purpose of our work to employ such setups to emulate and efficiently observe some of the well-known models and phenomena in condensed matter physics and quantum field theory by using the dark-state polaritons, where the polaritons are shown to follow the dynamics of quantum systems such as the Lieb-Liniger model, the Bose-Hubbard model, the quantum sine-Gordon model, the Fermi-Hubbard model, and the relativistic Thirring model. These quantum simulators provide a new platform in the field of understanding complex condensed matter

phenomena and quantum field models with currently accessible quantum optical techniques. The main tools used in our proposals involving stationary light-matter polaritons, condensed matter physics, and quantum field models, are textbook examples in the fields of quantum optics and strongly correlated systems. However, this inter-disciplinary combination can be used to resolve some of the long standing problems such as a direct observation of spin-charge separation, the correlations as witnesses of pinning transition and BCS-BEC crossover, and the realization of interacting Dirac particles in a continuous system, which have been proven undoubtedly difficult, and which have been demonstrated to be possible in our proposed schemes.

# List of Publications

## Publications:

[1] “Luttinger Liquid of Photons and Spin-Charge Separation in Hollow-Core Fibers”, D. G. Angelakis, M.-X. Huo, E. Kyoseva, and L. C. Kwek, *Phys. Rev. Lett.* **106**, 153601 (2011).

[2] “Sine-Gordon and Bose-Hubbard dynamics with photons in a hollow-core fiber”, M.-X. Huo, and D. G. Angelakis, *Phys. Rev. A* **85**, 023821 (2012).

[3] “Spinons and Holons with Polarized Photons in a Nonlinear Waveguide”, M.-X. Huo, D. G. Angelakis, and L. C. Kwek, *New J. Phys.* **14**, 075027 (2012).

[4] “Probing the BCS-BEC crossover with photons in a nonlinear optical fiber”, M.-X. Huo, C. Noh, B. M. Rodríguez-Lara, and D. G. Angelakis, *Phys. Rev. A* **86**, 043840 (2012).

[5] “Mimicking interacting relativistic theories with stationary pulses of light”, D. G. Angelakis, M.-X. Huo, D. Chang, L. C. Kwek, and V. Korepin, *Phys. Rev. Lett.* **110**, 100502 (2013).

## Preprints:

[1] “Interference Signatures of Abelian and Non-Abelian Aharonov-Bohm Effect on Neutral Atoms in Optical Lattices”, M.-X. Huo, W. Nie, D. Hutchinson, and L. C. Kwek, arXiv:1210.8008.

## Previous Publications in Other Directions:

[1] “The Photon-Like Flying Qubit in a Coupled Cavity Array”, M.-X. Huo, Y. Li, Z. Song, and C.-P. Sun, *Int. Journal of Quantum Inform.* **10**, 1250002 (2012).

[2] “Exact Results for the Criticality of Quench Dynamics in Quantum Ising Models”, Y. Li, M.-X. Huo, and Z. Song, *Phys. Rev. B* **80**, 054404 (2009).

[3] “The Peierls Distorted Chain as a Quantum Data Bus for Quantum State Transfer”, M.-X. Huo, Y. Li, Z. Song, and C.-P. Sun, *Europhys. Lett.* **84**, 30004 (2008).

[4] “Atomic Entanglement versus Visibility of Photon Interference for Quantum Criticality of a Hybrid System”, M.-X. Huo, Y. Li, Z. Song, and C.-P. Sun, *Phys. Rev. A* **77**, 022103 (2008).



# List of Figures

2.1	The ladder-, Vee-, and lambda-structure atoms . . . . .	10
3.1	The model setup for simulating sG and BH models . . . . .	23
3.2	The scheme for modulating the atomic density . . . . .	28
3.3	The Lieb-Liniger interaction parameter and the lattice depth	30
3.4	The phase diagrams for sG model and BH model . . . . .	33
3.5	The interaction and tunneling strengths . . . . .	35
3.6	The correlation functions for the polaritonic gas . . . . .	36
4.1	The model setup for simulating BCS-BEC-BB crossover . . .	41
4.2	The inter-species interaction and hopping strengths . . . . .	53
4.3	The correlation functions of polaritons . . . . .	55
4.4	The cross-species second-order correlations . . . . .	56
5.1	A schematic diagram of the spin-charge separation . . . . .	63
5.2	A schematic diagram of the system under consideration . . .	64
5.3	The model setup for simulating spin-charge separation with differently colored lights . . . . .	66
5.4	The Fourier transform of density-density correlation func- tion for the system with differently colored light . . . . .	72
5.5	The model setup for simulating spin-charge separation with differently polarized lights . . . . .	77
5.6	The Fourier transform of density-density correlation func- tion for the system with differently polarized lights . . . . .	83
6.1	The model setup for simulating Thirring model . . . . .	89
6.2	Regimes of bosonic and fermionic Thirring models . . . . .	95

6.3 The momentum cutoff and the log-scaled two-point correlations . . . . . 97

# List of Symbols

$\Psi$	polaritonic operator
$E$	field operator of quantum light
$\Omega$	Rabi frequency of classical light
$\sigma$	atomic operator
$n_z$	atomic density
$n_{\text{ph}}$	photonic density
$\Delta$	one-photon detuning
$\delta$	two-photon detuning
$g$	coupling strength between photon and atom
$k_Q$	wavevector of quantum light
$k_C$	wavevector of classical light
$\omega_Q$	central frequency of quantum light
$\omega_C$	central frequency of classical light
$v$	velocity of light in an empty medium
$v_g$	group velocity of light in a nonlinear medium
$m$	mass
$\chi$	interaction strength
$\Gamma$	total spontaneous emission rate
$\Gamma_{1D}$	spontaneous emission rate into the waveguide
$OD$	optical depth
$\eta$	single-atom cooperativity
$\gamma$	Lieb-Liniger parameter
$K$	Luttinger parameter



# Introduction

---

A one-dimensional (1D) system is typically formed by performing a tight confinement in its transverse directions, such that only the ground states in these directions need to be considered, and the particles only move and propagate along its longitudinal direction. The 1D systems is usually conceptually simple compared to its counterparts in two- and three-dimension. Several sophisticated approaches have been developed to solve some 1D systems exactly, such as the Bethe-ansatz method [1], while for other more complicated systems, methods like the Luttinger liquid theory have been introduced to solve them in the low energy domain [2]. In spite of the successful applications of these methods, complete knowledge about 1D systems remains elusive, such as the non-equilibrium evolutions and the behavior of correlation functions. To probe deeper into these elusive properties of 1D systems, the importance of system simulations becomes apparent. Along this line, numerical simulations using classical computers have been performed efficiently. One famous numerical approach to study 1D systems is the Density Matrix Renormalization Group (DMRG), where the main idea is to perform iterative diagonalizations in a reduced Hilbert space [3]. However, as the system size gets larger and larger, some problems become computationally intractable on classical computers. An alternative way is to study systems directly through quantum simulators. The basic idea is to use a well-controlled quantum system to simulate a desired quan-

tum system which is computationally difficult or experimentally inaccessible. The desired quantities are either detected or measured in a real experiment, where the uncharted regimes which are originally deemed impossible are explored and investigated.

The idea that a quantum system is best simulated with a quantum mechanical device stems from a seminal presentation by Richard Feynman thirty years ago [4]. However, at that time, the state of technology in manipulating cold atoms and molecules and constructing optical setups have not reached the current level of sophistication. Recent advances in technology, especially trapping technology, have demonstrated convincingly that such the possibility for a scalable quantum simulator could be achieved in the foreseeable future. In principle, quantum simulators are controllable quantum systems that could be used to simulate other quantum systems. They are essentially analog (quantum) computers capable of studying other quantum systems directly through measurements and observations. In some sense, they behave some primitive computer of nature [4, 5]. This direction also creates a motivation for the need to advance the current state of technology for cooling, addressing and manipulating atoms and molecules.

Many platforms for experimental realization of quantum simulators have been proposed and tested to some extent. Among the potential candidates for quantum simulators, the trapping of ultracold atomic gases in optical lattices has been widely used for a number of schemes, including the study of Mott transition from superfluid (SF) to Mott insulator (MI) phase [6, 7], the Tonks-Girardeau gas for strongly interacting bosons [8], the crossover from Bardeen-Cooper-Schrieffer (BCS) to Bose-Einstein condensate (BEC) in both fermionic and bosonic systems [9, 10, 11, 12, 13, 14, 15],

---

the realizations of field theory sine-Gordon (sG) [16] and Thirring models [17], and so on. While some marvelous achievements have been obtained experimentally for quantum simulations, there are still some inherent challenges in these schemes, for instance, fermionic atoms have been found to be difficult to cool to a sufficiently low temperature due to the existence of Pauli exclusion principle and measurements of certain correlations are still intractable despite advances in single-site addressing of atoms [18, 19].

A new research direction with strongly interacting dark-state polaritons through light-matter coupling has been proposed in recent years, where the polaritons are formed between the lower two stable levels of three-level atoms and resonant probe light in a nonlinear optical waveguide [20, 21, 22, 23, 24], based on a typical electromagnetically induced transparency (EIT) effect [21]. In the nonlinear waveguide case, the light beams are injected into a hollow-core waveguide doped with atoms [25, 26, 27, 28, 29, 30] or a nanofiber with atoms brought close to the surface of the fiber [31, 32]. A natural quasi 1D system is formed due to the tight-confinement of the waveguides. With a pair of counter-propagating classical control lasers in the waveguide, a weak quantum pulse is trapped as a standing wave formed by control lasers due to the Bragg scattering [22, 23, 24]. The principal differences between the quantum and classical lights are their frequencies and intensities. The classical lights are in orders of magnitude stronger and contain macroscopically large number of photons. They are also detuned from each other, by several GHz. This trapping allows enough time for polaritons to evolve according to like, e.g., the nonlinear Schrödinger equations of a designed system. During the evolution, the polaritons obey approximate bosonic statistics and can interact strongly with each other. After reaching the desired state, one of the con-

control lasers is turned off and the polaritons are released as outgoing photons. The photons continue to carry the information of polaritonic correlations, and the typical optical measurements on photons can give information on polaritonic correlations.

The nonlinear waveguide system can offer distinct advantages in enabling strong interactions between particles due to the tight field confinement and allowing for direct measurements of correlations. Based on this, we have proposed several schemes of quantum simulations using dark-state polaritons in the nonlinear waveguide [33, 34, 35, 36, 37]. These proposals include simulating pure bosonic features, and mimicking effective fermionic behaviors. In the latter case, we know that there is only a sign difference in the wavefunctions of hard-core bosons and fermions [38, 39]. When the studied features do not involve the sign difference, the hard-core bosons act effectively like the fermions [38, 39]. For instance, in the density-density correlations, the sign difference in the wavefunctions is squared such that the hard-core bosonic and fermionic systems share the same density-density correlation behaviors. In spite of the natural feature of a waveguide system, i.e., it is a continuous system, by superimposing an optical potential in the microwave regime, we have also created discrete polaritonic models [33, 34].

The strongly correlated models have been extensively investigated in the context of cold atoms in optical lattices [6, 7, 8, 15, 16, 17]. Motivated by these works, we explore the connection one step further to see if we could employ the light-matter systems which exhibit bosonic excitations, to simulate many-body phenomena. We show that in our case, the polaritons as dressed photons can be tuned to exhibit bosonic behavior on demand through the control lasers, and the intensities and correlations of polaritons



---

can be accessed with a high efficiency through standard optical techniques [33, 34, 35, 36, 37]. To start with our polariton-based simulations, we first introduce some basic knowledge, including the EIT effect [21], the light trapping techniques [22, 23, 24], the Lieb-Liniger model [40], the Luttinger liquid theory [2], and the correlations in 1D systems, in Chapter 2. After that, we describe our simulation schemes in the following Chapters.

In Chapter 3, we show that it is possible to impose an effective lattice potential on a single-species polaritonic gas and tune it to juxtapose between sine-Gordon and Bose-Hubbard models [33]. The sine-Gordon model is one of the well-known quantum field theory models starting from 1970s due to its soliton solutions [2], and the Bose-Hubbard model is a model describing interacting bosons in a lattice system [6]. The generation of the superimposed lattice is achieved through a slight modulation of atomic density.

Extending to a two-species polaritonic gas which is generated by utilizing two kinds of atoms and two quantum beams with different frequencies, in Chapter 4, we put the generated two-component polaritonic gas into two effective polaritonic lattice potentials to see the BCS-BEC crossover from a regime with weak attraction and pairing in momentum space (BCS regime) to a regime with strong attraction and pairing in real space (BEC regime) [34]. We begin with two types of four-level atoms interacting with two quantum lights and two control lasers. By tuning optical parameters, we make the intra-species interaction between the same-type polaritons extremely repulsive while keep the inter-species interaction between the different-type polaritons attractive. For infinite intra-species repulsion, the resulting model is mapped to an attractive Hubbard model by the Jordan-Wigner transformation, which allows us to study the BCS-BEC crossover

in the Hubbard model. The essential physics of the BCS and BEC limits, the long- and short-range spatial correlations, are readily attainable in our scheme by typical quantum optical techniques performed on photons.

We next discuss the possibility of the simulation of a two-component Luttinger liquid and a direct observation of the spin-charge separation in Chapter 5 [35, 36]. Although the spin-charge separation has attracted a lot of interest in condensed matter physics, its direct observation in experiments remains elusive. In our case, we first generate interactions between two polaritonic species. Then we derive the necessary intra- and inter-species terms by tuning the Rabi frequencies of the quantum and classical lasers, and their detunings from each atomic transition under consideration. When the terms achieve a required strength, we map the Lieb-Liniger model to a regime of spin-charge separation. Finally we analyze the possibility of directly accessing the velocities of the spin and charge waves in the Luttinger liquid. We introduce two schemes to simulate the two-component Luttinger liquid dynamics and the spin-charge separation, where in the first scheme we employ two quantum pulses with different frequencies interacting with two kinds of four-level atoms, and in the second scheme we utilize two oppositely circularly polarized quantum beams to interact with a single-type multi-level atomic gas. The quantum fields are weak coherent pulses containing a few photons (order of 10) initially. We would like to note the difference between these two schemes. In the first scheme, the parameters are relatively more flexible with less constraints, which allows for more complicated tasks of simulations. While for the advantage of the second scheme, it is easier to load one-species atoms and to distinguish two outgoing quantum lights with different polarizations.

In Chapter 6, we show that the interacting relativistic Dirac particles

---

in 1+1 dimensions can be generated with two kinds of differently polarized photons [37]. By storing and confining light pulses, and manipulating their dispersion relations and nonlinear interactions with nearby atoms, the light can behave effectively as either interacting bosonic or fermionic relativistic particles, and massive or massless, thus emulating the famous Thirring model from the quantum field theory. The realization of the Thirring model can demonstrate the famous mass renormalization due to the interactions. Typical quantum optical measurements collect the information on the scaling behavior of the correlation functions, and from that we can infer the properties of the model under consideration.



# Background

---

In this chapter, we will briefly review the basic tools from quantum optics and condensed matter physics which have been employed to develop the models of strongly correlated photons. According to the process of our simulations: generating the dark-state polaritons, achieving the desired regimes, and finally detecting the correlations, we will introduce the EIT nonlinearities and slow-light effect in the first section, review the basics of Lieb-Liniger model and Luttinger theories in the second section, and finally discuss the correlation functions in the third section.

## 2.1 Electromagnetic Induced Transparency and Dark-State Polaritons

The atom-doped nonlinear optical waveguides with well-controlled parameters, strong nonlinearities, and correlation accessing have provided a platform for studying condensed matter physics and quantum field models in a many-body context. The atoms are well trapped and manipulated by optical lasers, and their nonlinearity are enhanced by slowing light in the medium due to quantum interference mechanisms. One successful technique to slow light is based on the EIT effect, which is a quantum effect permitting the light propagation through an otherwise opaque medium [21]. It usually occurs in a system with three-level atoms and two optical pulses,

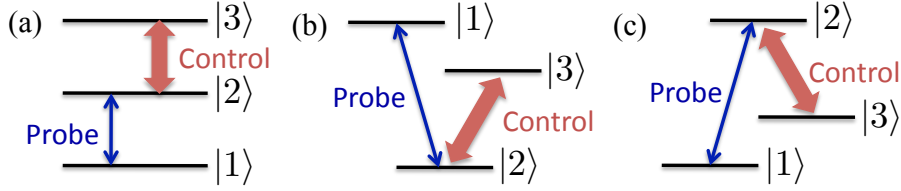


Figure 2.1: The (a) ladder, (b) Vee and (c) lambda structures of atoms. In each scheme, one of the three states is connected to the other two by the two optical fields: the probe and control fields. The three types of EIT schemes are differentiated by the frequency differences between this state and the other two. When the frequency difference (the sum for ladder system in (a)) between the probe and control fields matches the level splitting of the two un-coupled states, the otherwise opaque medium becomes transparent for the probe field.

one termed probe pulse and the other one called control or pump pulse. The atomic structure can be ladder, Vee or lambda (see Fig. 2.1), and the atoms are usually initialized in their ground states. In principle, the EIT effect originates from a destructive interference of two different transition paths. As shown in Fig. 2.1, we label these states as  $|1\rangle$ ,  $|2\rangle$ , and  $|3\rangle$ . A weak probe pulse is tuned to near resonant to the atomic transition  $|1\rangle \rightarrow |2\rangle$ , and a strong control field is tuned to near resonant to another transition  $|3\rangle \rightarrow |2\rangle$ . Next, we will focus on the lambda level in Fig. 2.1(c) as the EIT setup in the following. When the frequency difference between the probe and control fields is within the transparency window, the otherwise opaque medium becomes transparent for the probe pulse. At this time, the probe pulse can pass through the medium without any atomic absorption. Specifically, the probability amplitudes for the excitation of state  $|2\rangle$  come from two different driving paths:  $|1\rangle \rightarrow |2\rangle$  directly and  $|1\rangle \rightarrow |2\rangle \rightarrow |3\rangle \rightarrow |2\rangle$ . These two paths interfere destructively and allow a transparent window inside the  $|1\rangle \rightarrow |2\rangle$  absorption line.

The EIT effect can be used to slow and localize the probe pulse in the medium. As dictated by the Kramers-Kronig relation, a change in the

## 2.1. Electromagnetic Induced Transparency and Dark-State Polaritons

---

absorption over a narrow range of two-photon detuning must correspond to a change in the refractive index over a similarly narrow region, leading to an extremely low group velocity as  $v_g = c \tan^2 \theta$  with  $\tan^2 \theta = g^2 n / \Omega^2$  [41]. Here  $c$  is the speed of light in an empty waveguide,  $g$  is atom-field coupling strength proportional to the dipole matrix element of the  $|1\rangle \leftrightarrow |2\rangle$  transition,  $n$  is the atomic density, and  $\Omega$  is the Rabi frequency of the control laser. By adiabatically turning off the control laser, the probe amplitude will vanish and its state will be stored in a stationary atomic excitation.

This phenomenon can be well captured in the picture of dark-state polaritons, which are excitations coherently shared between light and atomic dark-state excitations:  $\Psi(z, t) = \Omega E(z, t) - \sqrt{n} g \sigma_{13}(z, t)$ . Here  $\Psi$  is the polariton operator,  $E$  is the quantum light operator, and  $\sigma_{13} = |1\rangle\langle 3|$  is the atomic operator. The so-called "dark-state" means that only meta-stable state is excited with no populations in higher excited states. Under certain conditions, the photons in the initial coherent quantum pulse will propagate in the medium as dark-state polaritons with a reduced group velocity [22, 23, 24].

In the slow-light scheme, a large ensemble of the atoms is initially prepared in the ground state. A weak quantum pulse, given by a coherent state, enters into the waveguide with a copropagating EIT control field from one side of the waveguide. By reducing the intensity of the control field, the quantum light is stored in stationary atomic excitations. Subsequently, in the form of a pure spin coherent wave, the excitation is stored and well protected from the environment for rather long times, and also stationary thus preventing any manipulation of its spatial shape. This atomic excitation can be converted back into a light pulse by turning on the control

laser, and the light pulse can then propagate in the direction of the control laser. To introduce an interaction between polaritons, a weak stationary retrieval field created by forward and backward control beams is adiabatically ramped up, where a small photonic component of the polariton is regenerated. By using forward and backward control fields, with time varying Rabi frequencies  $\Omega_+(t)$  and  $\Omega_-(t)$ , respectively, the weak pulse of signal light is manipulated [23]. The atomic coherence now is converted into a stationary photonic excitation. As the pulse-matching mechanism predicts, the quantum light becomes quasi-stationary to follow the oscillatory profile of the control fields. Specifically, if the two create a standing wave pattern, the EIT suppresses the signal absorption everywhere but in the nodes of the standing wave, resulting in a sharply peaked, periodic modulation of the atomic absorption for the signal light. Illumination with these beams also results in partial conversion of the stored atomic spin excitation into sinusoidally modulated signal light, but the latter cannot propagate in the medium owing to Bragg reflections off the sharp absorption peaks, leading to a vanishing group velocity of the signal pulse. It is sufficiently mobile for the polaritons to follow the profile of control fields although the photonic component is at all times very small. By introducing an additional fourth-level of atoms, the nonlinearity between polaritons is generated in such a stationary shape with a finite photonic component [42, 43].

## 2.2 Lieb-Liniger Model and Luttinger Liquid Theory

In 1D systems, the particles move along one direction, say  $z$  direction. Strong confinements in the transverse directions  $\mathbf{r}_\perp = \{x, y\}$  are applied



## 2.2. Lieb-Liniger Model and Luttinger Liquid Theory

---

such that only the lowest energy transverse quantum states  $\varphi_0(\mathbf{r}_\perp)$  need to be considered. The wavefunction of  $N$  particles reads as

$$\psi(\mathbf{r}_1, \dots, \mathbf{r}_N) = \psi(z_1, \dots, z_N) \prod_{i=1}^N \varphi_0(\mathbf{r}_{\perp,i}), \quad (2.1)$$

and usually we only consider  $\psi(z_1, \dots, z_N)$  for the study of the 1D system. For bosons with Dirac-delta interactions in a continuous system, they are described by the Lieb-Liniger model [40]

$$H = -\frac{1}{2m} \sum_{i=1}^N \frac{\partial^2}{\partial z_i^2} + \chi \sum_{i < j=1}^N \delta(z_i - z_j), \quad (2.2)$$

where  $m$  is the mass, and  $\chi$  is the interaction strength. As shown by Lieb and Liniger [40], this model is solvable using the Bethe ansatz method, where both the ground and excited states are attainable. However, in general, it is still very difficult to extract correlation functions from the solutions, while at the same time, correlation functions are very important because they are characteristic features of a quantum system. One alternative approach is to give a general description of the low energy sector of the above Lieb-Liniger model, where a liquid phase called Luttinger liquid appears [2]. In this phase, the low energy excitations are collective modes with a linear dispersion, and correlation functions exhibit an algebraic decay which is characterized by exponents that depend on the parameters of the model at zero temperature. The collective character of these low-energy excitations gives rise to a description in terms of collective fields called “bosonization” [2]. The bosonization method is used to approximately describe the low energy physics by a density-phase representation [2]. The reason of such a collective nature is that, with particle-particle interactions, one particle needs to push its neighbors away in order to propagate.

Therefore, when the confinement forces the particles moving along a line, any individual motion will be quickly converted into a collective one.

We express the bosonic field operators  $\psi$  and  $\psi^\dagger$  in the form of collective fields as

$$\psi(z) = e^{-i\theta(z)}[\rho(z)]^{1/2}, \quad (2.3)$$

$$\psi^\dagger(z) = [\rho(z)]^{1/2}e^{i\theta(z)}. \quad (2.4)$$

Here  $\rho(z) = \psi(z)^\dagger\psi(z)$  is the particle density, and  $\theta(z)$  is the phase. To see the quantum mechanical nature, we specify their commutation relations as

$$[\rho(z), \rho(z')] = 0, \quad (2.5)$$

$$[\theta(z), \theta(z')] = 0. \quad (2.6)$$

Together with

$$[\psi(z), \psi^\dagger(z')] = \delta(z - z') \quad (2.7)$$

for the bosonic field operators, we have

$$[\rho(z), e^{i\theta(z')}] = \delta(z - z')e^{i\theta(z')}. \quad (2.8)$$

Here the phase and density are canonically conjugated fields. We write the density operator  $\rho(z)$  as a combination of delta functions

$$\rho(z) = \sum_n \delta(z - z_n). \quad (2.9)$$

## 2.2. Lieb-Liniger Model and Luttinger Liquid Theory

---

With the expression for the delta function as

$$\begin{aligned}
\delta(z - z_n) &= \delta(z - \tilde{\phi}^{-1}(2n\pi)) \\
&= \delta(\tilde{\phi}^{-1}(\tilde{\phi}(z)) - \tilde{\phi}^{-1}(2n\pi)) \\
&= \frac{1}{\left|\frac{d\tilde{\phi}^{-1}(z)}{dz}\right|} \delta(\tilde{\phi}(z) - 2n\pi) \\
&= |\partial_z \tilde{\phi}(z)| \delta(\tilde{\phi}(z) - 2n\pi), \tag{2.10}
\end{aligned}$$

the density becomes

$$\rho(z) = |\partial_z \tilde{\phi}| \sum_n \delta(\tilde{\phi} - 2n\pi) = \frac{1}{2\pi} |\partial_z \tilde{\phi}| \sum_{m=-\infty}^{+\infty} \exp(im\tilde{\phi}), \tag{2.11}$$

where we have introduced a quantity  $\tilde{\phi}$  as  $\tilde{\phi}^{-1}(2n\pi) = z_n$ .

We continue to introduce another slowly varying quantum field operator as

$$\partial_z \tilde{\phi} = 2\pi\rho_0 + 2\partial_z \phi. \tag{2.12}$$

Substituting Eq. (2.12) into Eq. (2.11), the density operator becomes

$$\rho(z) = \left(\rho_0 + \frac{1}{\pi} \partial_z \phi\right) \sum_{m=-\infty}^{+\infty} \exp[im(2\pi\rho_0 z + 2\phi)]. \tag{2.13}$$

When  $\rho(z)$  varies slowly, we can only keep the lowest frequency component with  $m = 0$  for it:

$$\rho(z) \simeq \rho_0 + \frac{1}{\pi} \partial_z \phi(z). \tag{2.14}$$

Going back to Eq. (2.8) about the commutation relation of  $\rho(z)$  and  $e^{i\theta(z')}$ , we have

$$\left[\theta(z), \frac{1}{\pi} \partial_z \phi(z')\right] = i\delta(z - z'). \tag{2.15}$$

For the one-component Lieb-Liniger model, the Hamiltonian is

$$H = \int dz \left[ \frac{1}{2m} \partial_z \psi(z)^\dagger \partial_z \psi(z) + \frac{\chi}{2} \rho^2(z) \right]. \quad (2.16)$$

Going beyond this simple case, novel physics can be obtained by considering two-component bosons or two internal degrees of freedom of bosons, where the Hamiltonian of this two-component Lieb-Liniger model is given by

$$H = \int dz \left[ \sum_s \left( \frac{1}{2m_s} \partial_z \psi_s^\dagger \partial_z \psi_s + \frac{\chi_s}{2} \rho_s^2 \right) + \chi_{\uparrow\downarrow} \rho_\uparrow \rho_\downarrow \right]. \quad (2.17)$$

Here the field operator  $\psi_s$  and the density operator  $\rho_s$  with  $s = \uparrow, \downarrow$  correspond to two species of bosons with a mass  $m_s$ , an intra-species interaction strength  $\chi_s$ , and an inter-species interaction strength  $\chi_{\uparrow\downarrow}$ .

## 2.3 Correlation Functions

The first-order correlation of a signal pulse  $\hat{E}(z, t)$

$$g^{(1)}(z, z'; \tau) = \int_{-\infty}^{\infty} \hat{E}(z, t) \hat{E}^*(z', t - \tau) dt \quad (2.18)$$

describes the similarity between observations as a function of time and separation between them. In experiments, correlation functions are expected to be readily detected by placing a detector at the output of a Michelson interferometer, where the detector is illuminated by the input field  $\hat{E}(z, t)$  coming from one arm, and by the delayed replica  $\hat{E}(z', t - \tau)$  from the other arm. If the time response of the detector is much larger than the time duration of the signal  $\hat{E}(z, t)$ , or if the recorded signal is integrated,

### 2.3. Correlation Functions

---

the detector measures the intensity  $A_M$  as the delay  $\tau$  is scanned:

$$A_M(\tau) = \int_{-\infty}^{\infty} |\hat{E}(z, t) + \hat{E}(z', t - \tau)|^2 dt. \quad (2.19)$$

Expanding  $A_M(\tau)$  reveals that one of the expanded terms is the field correlation

$$g^{(1)}(z, z'; \tau) = \int_{-\infty}^{\infty} \hat{E}(z, t) \hat{E}^*(z', t - \tau) dt. \quad (2.20)$$

At this time, the momentum distribution can also be easily constructed by taking the Fourier transform of the correlation  $g^{(1)}$ .

For the second-order correlation

$$g^{(2)}(z, z'; \tau) = \frac{\langle I(z, t) I(z', t - \tau) \rangle}{\langle I(z, t) \rangle \langle I(z', t - \tau) \rangle}, \quad (2.21)$$

we can detect it by measuring the intensity correlation

$$g^{(2)} \langle I(z, t) \rangle \langle I(z', t - \tau) \rangle = \int_{-\infty}^{\infty} I(z, t) I^*(z', t - \tau) dt. \quad (2.22)$$

Here  $I(z, t) = |\hat{E}(z, t)|^2$  is the intensity of the pulse  $\hat{E}(z, t)$  up to a constant in the conventional definition of intensity. Similar to the above setup to measure the field correlation, two parallel beams with a variable delay are generated, and then focused into a second-harmonic-generation crystal to give a signal proportional to  $|\hat{E}(z, t) + \hat{E}(z', t - \tau)|^2$ . Only the beam propagating on the optical axis, proportional to the cross-product  $\hat{E}(z, t) \hat{E}(z', t - \tau)$ , is retained. This signal is then recorded by a detector, which measures

$$A_M(\tau) = \int_{-\infty}^{\infty} |\hat{E}(z, t) \hat{E}(z', t - \tau)|^2 dt = \int_{-\infty}^{\infty} I(z, t) I(z', t - \tau) dt. \quad (2.23)$$

We note here that  $A_M(\tau)$  is exactly the intensity correlation

$$g^{(2)}\langle I(z, t)\rangle\langle I(z', t - \tau)\rangle = \int_{-\infty}^{\infty} I(z, t)I^*(z', t - \tau)dt. \quad (2.24)$$

In our system, the correlations are obtained by turning off one of the control lasers and performing the above described measurements on the outgoing photons. For the quantum optical simulation of models and phenomena in many-body physics, the attainability of correlations is significant. This is because that the large number of results on 1D systems can be roughly divided in two main classes. One is the exact results based on the Bethe ansatz analysis. While they are rigorous and give very non trivial information on the spectrum, it is essentially difficult to compute the correlations, which are the quantities directly related to the physical observables. Even if one has the full form of the wave functions (what is actually not the case as the Bethe ansatz gives the wave functions as the solutions of complicated integral equations), computing the correlations from them is essentially impossible. Furthermore, as they rely on delicate integrability properties of the system, they are not robust when there are modifications of the model, such as extensions to two components or nonlocal but short-ranged interactions. Beyond the exact solutions, a combination of techniques including numerical simulations, bosonization, and Renormalization Group gives information on correlations. However, these results are generally not rigorous. For instance, the first- and second-order correlations of a Luttinger liquid are given by [2]:

$$g^{(1)} \sim 1/(z - z')^{2K} \quad (2.25)$$

### 2.3. Correlation Functions

---

and

$$g^{(2)} \simeq I^2 + \frac{cK}{(z - z')^2} + \frac{c' \cos(2\pi I(z - z'))}{(z - z')^{2K}} \quad (2.26)$$

with the Luttinger parameter  $K$  and two constants  $c$  and  $c'$ .

